

# Influence of alumina/MWCNT hybrid nanoparticle additives on tribological properties of lubricants in turning operations

Anuj Kumar SHARMA\*, Jitendra Kumar KATIYAR, Shubrajit BHAUMIK, Sandipan ROY

*Tribology and Surface Interaction Research Lab, Department of Mechanical Engineering, SRM Institute of Science and Technology Kattankulathur, Tamil Nadu 603203, India*

*Received: 26 September 2016 / Revised: 31 October 2017 / Accepted: 17 November 2017*

© The author(s) 2018. This article is published with open access at Springerlink.com

**Abstract:** A hybrid lubricant with improved thermal and tribological properties was developed by blending multiwalled carbon nanotubes (MWCNTs) with alumina-based nanoparticles into cutting fluid at fixed volumetric proportions (10:90). The hybrid cutting fluid was prepared in different volumetric concentrations (0.25, 0.75, and 1.25 vol%), and the tribological properties and contact angles were measured using pin-on-disc tribometry and goniometry, respectively. The study showed a reduction in wear and friction coefficient with increasing nanoparticle concentration. The cutting fluid performance was investigated using minimum quantity lubrication (MQL) in the turning of AISI 304 stainless steel. Regression models were developed for measuring the temperature and tool flank wear in terms of cutting speed, feed, depth of the cut, and nanoparticle concentration using response surface methodology. The developed hybrid nanolubricants significantly reduced the tool flank wear and nodal temperature by 11% and 27.36%, respectively, as compared to alumina-based lubricants.

**Keywords:** hybrids; nanolubricants; MQL; MWCNT; tool wear; friction coefficient

## 1 Introduction

In the manufacturing industry, the high heat generation in the machining zone restricts the cutting speed of tools during the dry machining of steel. Hence, the desired surface finish is never fully achieved in high speed machining under dry cutting conditions. Furthermore, the high heat affects the hardness and sharpness of the cutting tools causing premature breakage. To overcome these issues, appropriate cutting fluids need to be included in high-speed machining. Cutting fluids play vital role in cooling and lubricating the cutting tool's work-piece interfaces, and at washing away chips from the machining zone. The conventional way of cooling is effective but their excessive use pollutes the environment and may be hazardous for the human.

To restrict excessive use of conventional cutting

fluids MQL/NDM (near dry machining) has appeared to improve the penetration of the lubricant into the machining zone. In this technique, a small quantity of cutting fluid is sprayed into the cutting zone under pressurized air. Maruda et al. [1] showed that the minimum quantity lubrication (MQL) technique is suitable for spraying cutting fluid into the cutting zone. Furthermore, Attanasio et al. [2] used the MQL technique and observed reduction of the wear rate of the cutting tools as compared to dry machining method. Research groups by Maruda et al. [3], Cantero et al. [4] and Klocke et al. [5] showed that the use of the MQL technique improves the surface finish and tool life, and reduces the machining forces. Moreover, Maruda et al. [6] achieved a reduction of 40% in tool wear using the minimum quantity cooling lubrication (MQCL) technique. A study on the hybridized MQL with cryogenic cooling by Sartori et al. [7] showed

\* Corresponding author: Anuj Kumar SHARMA, E-mail: anujkumar.s@ktr.srmuniv.ac.in

better results compared to conventional flood lubrication technique. According to the authors, MQL can be a viable alternative for wet machining because it may minimize both the manufacturing costs and the environmental hazards.

The conventional fluids have good lubrication properties but their poor thermal properties restrict them to be used as cutting fluids. The thermal conductivity of the conventional fluids, which is related to the heat extraction capability, may increase after mixing particles with sizes in the millimeter to micrometer range. However, the use of micron-sized particles leads to clogging and poor stability of the suspensions. To overcome this, the nanoparticles of the nm size range have replaced the micron-sized particles, leading to the synthesis of a new generation of fluids called “nanofluids”.

Numerous researchers observed an increase in the nanofluid thermal conductivity with an increase in the nanoparticle concentration in a base fluid [8–10]. Furthermore, a 22.4% increase in thermal conductivity was observed after mixing 6%  $\text{Al}_2\text{O}_3$  in a base fluid at ambient temperature, as compared to conventional fluids [11]. Yang [12] and Choi et al. [13] also observed an increase of about 200% and 150% in thermal conductivity, respectively, when multiwalled carbon nanotubes (MWCNT) were added to the base fluid.

Besides the thermal conductivity of the cutting fluid, the friction between the tool and the work-piece interface plays a critical role in the heat generation of the machining zone. The friction increases the tool tip temperature resulting in decrement of the hardness and sharpness of the tool's cutting edge. Hence, friction affects significantly the surface finish and aggravates the tool wear. Sharma et al. [14] showed that the mixing of nanoparticles with cutting fluid increased the thermal conductivity resulting in increased tool life, whereas the cutting force, surface roughness, and cutting temperature decreased. Studies showed that blending of graphite nanoparticles with base fluid enhances its tribological properties because of the lower friction coefficient [15], while  $\text{MoS}_2$  and graphite solid lubricants reduce the surface roughness and the cutting force during machining [16]. Researchers also observed improved surface quality and reduction of the tool wear, cutting force, and chip thickness

compared to dry and conventional wet machining [17, 18]. Additionally, Amrita et al. [19] showed that MQL method reduced the surface roughness, cutting force, cutting temperature and tool wear by 30%, 54%, 25% and 71%, respectively in comparison to conventional wet machining. Yasar et al. [20] observed a reduction in the temperature of the cutting tool during machining with the use of oil based  $\text{TiO}_2$  nanofluid. Paras et al. [21] noticed an enhancement of the tribological properties of conventional lubricants after mixing  $\text{CuO}$  and alumina nanoparticle additives. Roy and Ghosh [22] found that 1 vol% of MWCNTs and 3 vol% of alumina noticeably reduced the specific energy and cutting force. Furthermore, mixing  $\text{ZnO}$  and  $\text{WS}_2$  nanoparticles with conventional lubricants increased the tribological properties [23].

So far, researchers focused on lubricants containing mono-type nanoparticles in machining. Very few studies [8, 18, 24–30] have been found on hybrid nanofluids, such as colloidal suspensions enriched with two different types of nanoparticles. A review on hybrid nanofluids by Sarkar and Ghosh [24] indicated that a proper hybridization may be contribute to creating hybrid nanofluids for potential use in heat transfer enhancement. Tansen et al. [25] reported that the addition of a small amount of MWCNT nanoparticles to water-based alumina solution increased its potential as a heat transfer fluid. Furthermore, Nine et al. [26] achieved a significant improvement in thermal conductivity by mixing MWCNT nanoparticles with alumina nanofluids, whereas Ahammed et al. [27] recorded an increase of 88.62% in convective heat transfer coefficient and a reduction of 4.7 °C in temperature using alumina-graphene hybrid nanofluids. Zhang et al. [28] used  $\text{MoS}_2$ -CNT hybrid nanofluids in grinding and yielded lower G ratio and surface roughness compared to  $\text{MoS}_2$  and CNT nanofluids. Moreover, studies on the hybridization of different types of nanoparticles showed an enhancement in thermophysical [29] and tribological [30] properties of base nanofluids. However, the use of hybrid nanofluids as cutting fluids in machining and in turning operations has not been reported.

In the present study, a hybrid nano-lubricant was developed by mixing MWCNT nanoparticles with alumina-based nanofluids in different nanoparticle

concentrations (0.25%, 0.75%, and 1.25%). The optimization of the nanoparticle concentration was performed using response surface methodology (RSM) and regression models for tool wear and temperature dependence were developed. The evaluation of the formed hybrid nanolubricants as cutting fluid in turning of AISI 304 stainless steel was conducted for nodal temperature and tool flank wear using the MQL technique. The results were compared with those from the machining performance of alumina-based nanofluids.

## 2 Experimental details

### 2.1 Preparation of nanolubricants

The base fluid was prepared by mixing 5 vol% vegetable oil in distilled water. The detergent was used as an emulsifier in 0.5 vol% concentration to stabilize the emulsion of the base fluid. The hybrid ( $\text{Al}_2\text{O}_3/\text{MWCNT}$ ) nanofluid was prepared by mixing  $\text{Al}_2\text{O}_3$  nanofluid (colloidal suspension containing 23% of  $\text{Al}_2\text{O}_3$  nanoparticles, 45 nm in diameter purchased by Alfa Aesar<sup>®</sup>) with MWCNT nanoparticles in a volumetric ratio of 90:10 in the base fluid at three volumetric concentrations (0.25, 0.75, and 1.25 vol%). The surfactant cetyltrimethylammonium bromide (CTAB) was already added to the suspension by the manufacturer. The prepared nanofluids were kept in an ultrasonicator (Toshiba, India) generating 100 W ultrasonic pulses at  $36 \pm 3$  kHz at a stretch for 6 h until a homogeneous and stable suspension was achieved. A fresh nanocutting fluid sample was prepared for each measurement and was used immediately to avoid possible agglomeration or sedimentation. Figure 1 shows the TEM images of nanofluids verifying the size and monodispersity of

the nanoparticles.

### 2.2 Thermal conductivity

The thermal conductivity of the alumina and Al-MWCNT nanofluid samples was measured at five temperatures: 25, 35, 40, 45, and 50 °C. A transient hot wire apparatus (Decagon Devices, Inc., USA) was used to measure the thermal conductivity and thermal resistivity for the rate of temperature increase of the probe at a constant heating rate. To improve accuracy, a KD2 Pro probe was attached vertically to a table. The minimum amount of nanofluid required for measuring the thermal conductivity was 45 mL. The probe was submerged into the fluid sample for approximately 15 min prior to the first measurement. To achieve thermal equilibrium successive measurements were done every 15 min. The effect of nanoparticle concentration on the thermal conductivity was also studied.

### 2.3 Tribological testing

The nanofluid samples were tested for their tribological behavior with a pin-on-disc tribometer TR-20 (Ducom, India) with maximum speed and load capacity of 2,000 rpm and 1,000 N, respectively. The experimental set-up is depicted in Fig. 2. A cylindrical pin ( $\varphi$  3 mm  $\times$  40 mm) and a disc (diameter 155 mm) that were used in this experiment were both made of AISI 304 stainless steel. The linear speed and load were kept constant at 1 m/s and 40 N, respectively. Each experiment run time was 300 s. The sliding track of pin was changed after each run to ensure the availability of a virgin surface for the next run. The rpm of the disc was varied to maintain constant sliding speed and the disc was cleaned after each run with acetone to remove any debris.

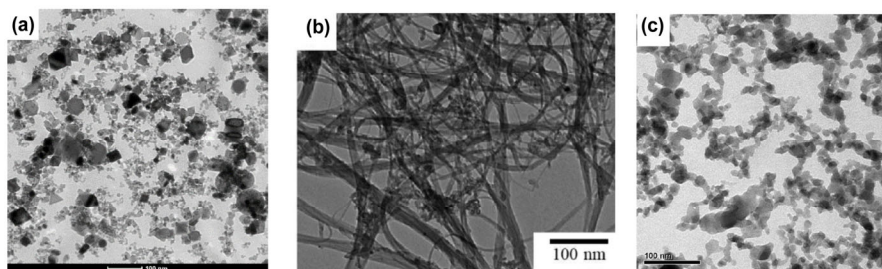


**Fig. 1** TEM images of (a) alumina, (b) MWCNT nanofluid, and (c) Al-MWCNT hybrid nanofluid.



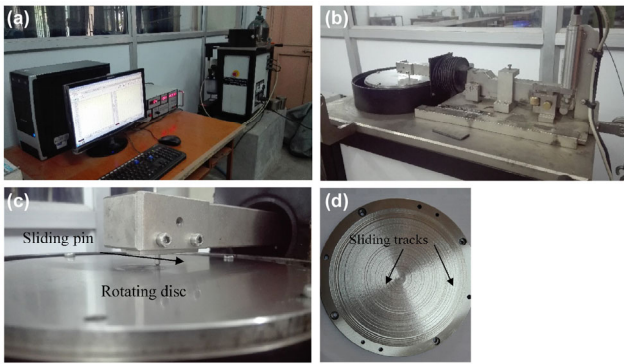


**Fig. 2** (a) Pin-on-disc experimental setup; (b) pin and disc machine; (c) closed view of sliding pin on rotating disc; (d) sliding tracks on rotating disc.

#### 2.4 Wettability testing of the nanofluids

The spreadability of the lubricant over the tool surface enhances the available surface area for the heat extraction on hot tool surfaces. The contact angle measurement is based on the Young's equation (Eq. (1)) [31] which describes an equilibrium force balance at three phase interfaces (solid tool, liquid lubricant, and air) as illustrated in Fig. 3(b). The equilibrium thermodynamic contact angle ( $\theta$ ) is given by the equation:

$$\cos \theta = \frac{\sigma_{sv} - \sigma_{sl}}{\sigma_{lv}} \quad (1)$$

where  $\sigma_{lv}$ ,  $\sigma_{sv}$ , and  $\sigma_{sl}$  is the liquid-vapor, solid-vapor, and solid-liquid interfacial tensions, respectively.

The contact angle ( $\theta$ ) was measured at different nanoparticle concentrations (from 0 to 1.5%) using a drop shape analyzer 25 (provided by KRUSS), as shown in Fig. 3. The carbide insert was kept on the work-table at ambient temperature and allowed to reach equilibrium at a saturated relatively humid environment. Afterwards, 10  $\mu\text{L}$  of the lubricant was carefully dropped through a 0.5 mm OD needle tip

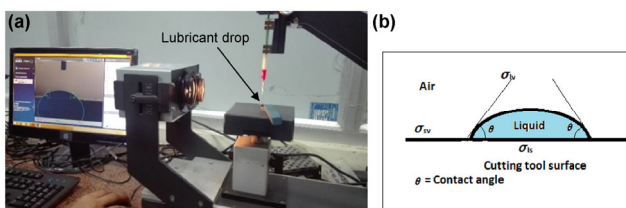


**Fig. 3** (a) Contact angle measurement setup; (b) schematic diagram showing a liquid droplet on solid surface.

on the top surface of the carbide insert. A camera captured the image of a drop pendant that was formed on the tool surface, and the inbuilt software measured the contact angle. Each experiment was conducted thrice for every sample and their average was considered as the final reading.

#### 2.5 Experimental set-up of turning

The turning of AISI 304 stainless steel was performed using the MQL technique on a HMT (model NH 22/1500) lathe machine under mist of alumina and Al-MWCNT nanofluids. A coated cemented carbide insert (Widia's CCMT 09T304-TN2000) was mechanically clamped on a rigid tool holder (widax SCLCR1212F09 D 3J) and was used as cutting tool. The MQL operating fixed parameters included the fluid flow rate at 2.5 mL/min and the air supply pressure at 4 bar. A discharge nozzle, capable of impinging mist vertically downward on the tool, was placed at 5 cm distance above the rake face of the cutting tool (Fig. 4(b)). The mist of the synthesized nanocutting fluid fell naturally on the cutting zone. After each experiment, the carbide insert was removed and dried, and its primary flank wear was evaluated using an Olympus BX51M microscope with a 10 $\times$  lens. For better understanding of the process the micrographs had a 200  $\mu\text{m}$  scale.

To measure the nodal temperature of the junction

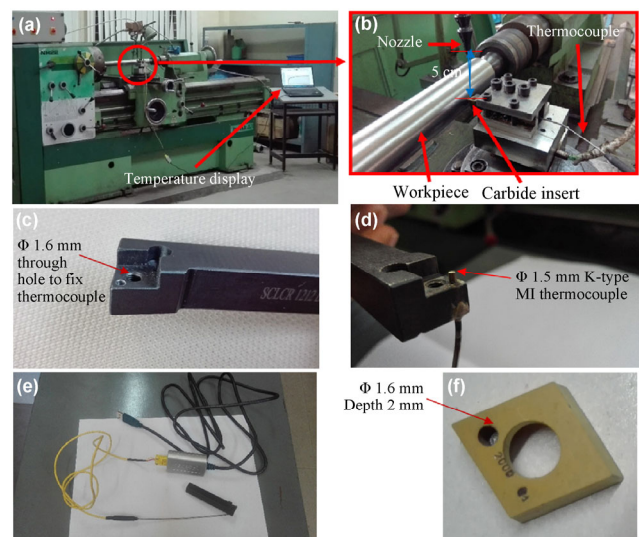


**Fig. 4** (a) Turning experimental setup; (b) machining zone close view; (c) tool holder with drilled hole; (d) tool holder fitted with thermocouple; (e) USB TC-01 NI DAQ system; (f) carbide tool insert with drilled hole.

between the thermocouple and the tool we developed an *in-situ* set-up consisting of a metal insulated (MI) K-type thermocouple embedded in the tool holder and connected to the computer system through National Instruments data acquisition system USB-TC01 (Fig. 4). To reach closer to the tool tip, a hole of 1.6 mm diameter was drilled through the tool holder (Fig. 4(c)) and the carbide tool was inserted to a depth of 2 mm (Fig. 4(f)). The MI K-type thermocouple of sheath diameter 1.5 mm was inserted and fixed in the tool holder with a silver brazing (Fig. 4(d)). This in-house developed set-up was used to record the nodal temperature during turning operations of the alumina and Al-MWCNT nanofluids. Each experiment was conducted thrice and the average value was considered.

## 2.6 Experimental design

The response surface methodology (RSM) is the collection of statistical techniques used for the modeling and analysis of problems at which one or more responses of interest are influenced by several variables. The RSM focuses on the relationship between multiple independent variables and the response variable ( $y$ ), expressed as below:

$$y = f(x_1, x_2, x_3, \dots, x_k) \quad (2)$$

where  $f$  is a multivariate function and  $(x_1, x_2, x_3, \dots, x_k)$  represent the independent variables (factors). This relationship describes a curved surface known as the response surface. When the first-order lacks in providing an acceptable fit, due to the interaction between the variables and the surface curvature, a second-order model is used to improve the optimization process. A general second-order model is defined as:

$$y = a_0 + \sum_{i=1}^n a_i x_i + \sum_{i=1}^n a_{ii} x_i^2 + \sum_{i=1}^n \sum_{j=1}^n a_{ij} x_i x_j, \quad i < j \quad (3)$$

where  $a_0$  is a constant,  $a_i$ ,  $a_{ii}$ , and  $a_{ij}$  are the coefficient of the first-order (linear), second-order (quadratic), and cross-product terms, respectively, and  $x_i$  and  $x_j$  represent the input variables.

The optimization of the input variables were done by RSM using a Box-Behnken design to get the optimized value of the response variables. A total number of 27 trials, including three center points,

were employed. All the experiments were performed independently thrice, and the average value of each response was considered. The process variables (input machining parameters) and their values at different levels are listed in Table 1. We used the Design-Expert 10.0 software to design the Box-Behnken experimental set-up, and to perform the regression analysis of the experimental data, build the quadratic model, and plot the three-dimensional response surface plots. The analysis of variance (ANOVA) was evaluated with a statistical analysis of the models. The fitting quality of the second-order polynomial model equation was considered statistically via the determination coefficient ( $R^2$ ) and the adjusted  $R^2$ . The fitted polynomial equation, expressed by three-dimensional surface plots, was used to evaluate the relationship between the response variables and visualize the interaction between the variables used in this study. A point optimization method optimized the level of each variable for a desirable response. A combination of different optimized input variables, which yielded the desired value of the response, was chosen to verify the validity of the model. Finally, validation experiments tested the adequacy of the experimental set-up. Table 2 shows the experimental design for the alumina and its hybrid nanofluid (alumina-MWCNT) with each run order and the machining performance in terms of the nodal temperature ( $T$ ) and the tool flank wear (VB).

## 3 Results and discussion

### 3.1 Characterization of nanofluids

Figure 5 shows the thermal conductivity of the nanofluids as a function of temperature at various volumetric concentrations. It was found that the thermal conductivity of all nanofluids increased with increase in both the nanoparticle volumetric concentration and temperature. The highest thermal conductivity was

**Table 1** Control factors and their levels.

Control factor	Symbol	Units	Level 1	Level 2	Level 3
Cutting speed	$v$	m/min	60	90	120
Feed rate	$f$	mm/rev	0.08	0.12	0.16
Depth of cut	$d$	mm	0.6	0.9	1.2
Nanoparticle concentration	$np$	vol%	0.25	0.75	1.25

**Table 2** Experimental results for  $T$  and  $VB$  using Alumina ( $Al_2O_3$ ) and Al-MWCNT hybrid nanofluid.

Run	Machining parameters				Response variables			
					Alumina nanofluid		Al-MWCNT nanofluid	
	$v$ (m/min)	$f$ (mm/rev)	$d$ (mm)	$np$ (vol%)	$T$ ( $^{\circ}C$ )	$VB$ ( $\mu m$ )	$T$ ( $^{\circ}C$ )	$VB$ ( $\mu m$ )
1	90	0.16	1.2	0.75	246.1	195.66	212.675	170.14
2	60	0.12	1.2	0.75	201.6	176.16	191.475	153.18
3	120	0.12	0.9	1.25	205.4	171.72	190.65	149.32
4	60	0.12	0.6	0.75	155.3	123.44	134.175	107.34
5	90	0.12	0.9	0.75	190.3	151.27	164.425	131.54
6	60	0.12	0.9	0.25	225.3	179.13	194.675	155.74
7	120	0.12	1.2	0.75	249.8	198.57	215.838	172.67
8	120	0.08	0.9	0.75	183.2	125.82	167.313	133.85
9	90	0.08	1.2	0.75	186.7	148.42	161.325	129.06
10	60	0.08	0.9	0.75	149.5	118.84	129.175	103.34
11	90	0.12	0.9	0.75	185.8	147.72	160.563	128.45
12	120	0.12	0.9	0.25	189.4	166.06	163.7	130.96
13	90	0.12	1.2	1.25	219.8	156.41	189.963	151.97
14	90	0.12	0.9	0.75	197.2	156.75	170.387	136.31
15	60	0.16	0.9	0.75	217.5	161.93	169.9	135.92
16	120	0.12	0.6	0.75	127.1	137.25	109.863	87.89
17	90	0.12	0.6	0.25	142.6	113.37	123.225	98.58
18	90	0.08	0.6	0.75	81.5	64.82	70.4625	56.37
19	90	0.08	0.9	0.25	168.8	134.18	145.85	116.68
20	90	0.08	0.9	1.25	154.2	122.57	95.725	76.58
21	60	0.12	0.9	1.25	141.8	144.51	132.063	105.65
22	90	0.12	1.2	0.25	231.6	184.16	200.175	160.14
23	90	0.12	0.6	1.25	135.9	88.06	117.463	93.97
24	90	0.16	0.6	0.75	148.5	118.06	128.325	102.66
25	90	0.16	0.9	1.25	207.7	165.13	179.512	143.61
26	90	0.16	0.9	0.25	219.9	174.81	190.012	152.01
27	120	0.16	0.9	0.75	223.1	186.23	225.287	180.23

observed at the highest temperature ( $50^{\circ}C$ ) at concentration 1.25 vol% for the Al-MWCNT hybrid nanofluids. It was shown that blending of MWCNT with alumina enhanced the thermal conductivity ( $\sim 2.6\%$ ). The obtained results are in good agreement with previous investigations [25, 26, 31].

The images of drop pendants for the alumina and the Al-MWCNT hybrid nanofluids at different concentrations are depicted in Figs. 6 and 7, respectively. The results show that the wettability (expressed as

the contact angle) of the nanocutting fluids is affected significantly by the nanoparticle concentration. Specifically, the contact angle of alumina and its hybrid nanofluid decreases and then increases as the nanoparticle concentration increases from 0.25 up to 1.5 vol%. Similarly, Wasan et al. [32] observed an increase in the contact diameter (spreading) of the droplet with increasing nanoparticle concentration in conventional fluids. The smallest contact angle, giving maximum wetting area per unit liquid volume,

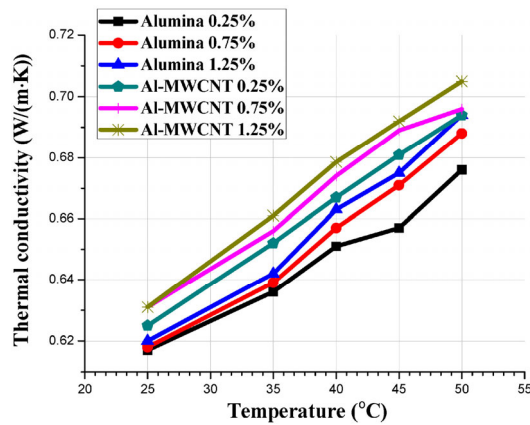


**Fig. 5** Thermal conductivity of alumina and Al-MWCNT hybrid nanofluid samples at different temperatures.

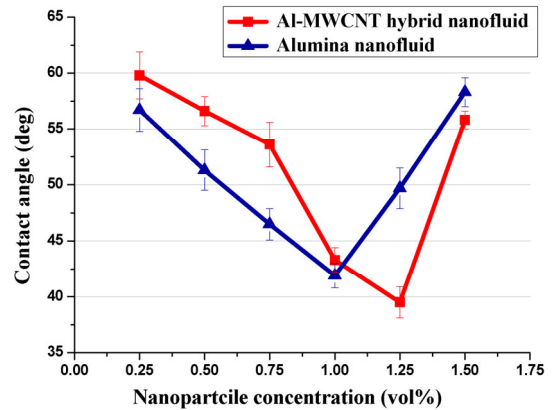


**Fig. 7** Contact angle for alumina and Al-MWCNT hybrid nanofluid samples at different concentrations.

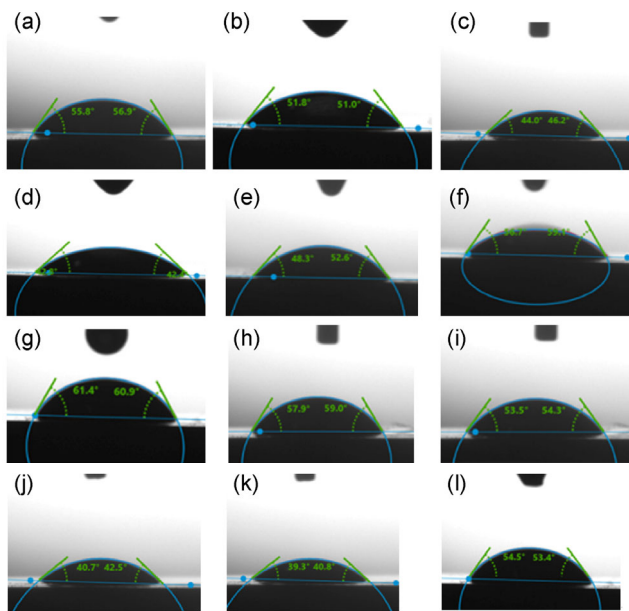


**Fig. 6** Examples of drop pendants on carbide tool surface for Alumina nanofluid (a) 0.25 vol%, (b) 0.5 vol%, (c) 0.75 vol%, (d) 1.0 vol%, (e) 1.25 vol%, (f) 1.5 vol%, and for Al-MWCNT hybrid nanofluid (g) 0.25 vol%, (h) 0.5 vol%, (i) 0.75 vol%, (j) 1.0 vol%, (k) 1.25 vol%, (l) 1.5 vol%.

was recorded at 39.5° (1.25 vol%) and 41.9° (1.0 vol%) for the Al-MWCNT and alumina nanofluids, respectively. Hence, the addition of MWCNT to alumina-based nanofluids improved their wettability, and enhanced their heat extraction and lubricating properties. These findings are in good agreement with results obtained previously [31, 32]. Figure 8 shows that the Al-MWCNT hybrid nanofluids exhibit lower friction coefficient between the pin and the disc compared to alumina nanofluids. A friction coefficient of approximately 0.07 and 0.18 was measured for

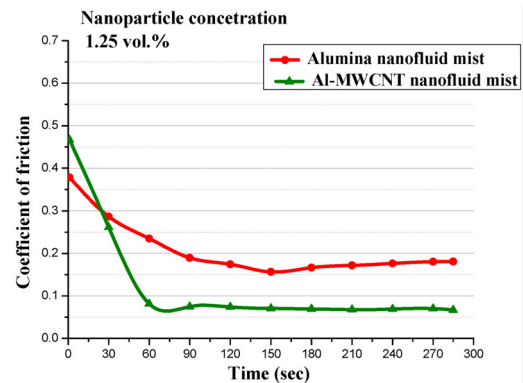


**Fig. 8** Variation in coefficient of friction for alumina and Al-MWCNT hybrid nanofluid at 1.25 vol% concentration as a function of time.

Al-MWCNT and alumina-based nanofluids, respectively, at 1.25 vol%. A lower value of friction coefficient reduces the friction force and therefore reduces the pin wear. The average pin wear was determined as ~481, ~273, and ~198 μm for Al-MWCNT hybrid nanofluid and ~494, ~403, and ~387 μm for alumina based nanofluids at concentrations 0.25, 0.75 and 1.25 vol%, respectively. The lowest wear value (~198 μm) was recorded at 1.25 vol% for the Al-MWCNT hybrid nanofluids. Moreover, a reduction in wear was observed with increase of the nanoparticle concentration for both, the alumina and its hybrid nanofluids (Fig. 9). This may be attributed to the formation of a nanolayer between the sliding surface of the pin and the disc. Furthermore, the intensity of the mono-layer could be enhanced by the increased number of nanoparticles at higher concentrations. Field emission scanning electron microscope (FESEM) images are shown in Fig. 10 for various nanofluid samples. The images



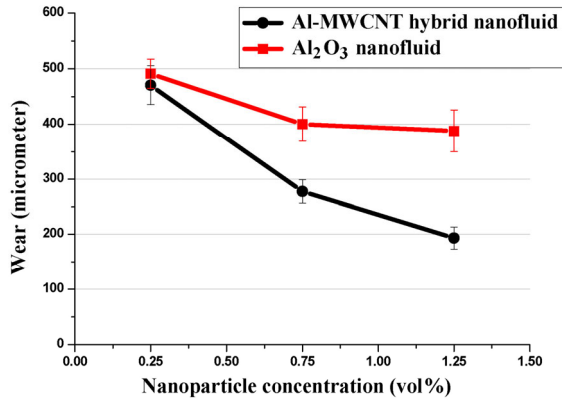


**Fig. 9** Wear measurement for alumina and Al-MWCNT hybrid nanofluid samples at different concentrations.

were taken at the sliding surface of the pin during the pin-on-disc experiment with a magnification of 1.00 KX. A significant difference in the surface quality was

observed for different nanofluids and base fluids. The poor quality surface and the sliding marks are clearly visible at the image of the alumina nanofluid sample. It was also observed that the Al-MWCNT hybrid nanofluids had the smoothest surface, suggesting that the hybrid nanofluids are superior lubricants compared to the alumina nanofluids. Furthermore, improved surfaces were observed at the optimized nanoparticle concentrations for both types of nanofluids (alumina and Al-MWCNT hybrid).

### 3.2 Turning of alumina (Al<sub>2</sub>O<sub>3</sub>) and alumina-MWCNT mixed nanoparticle nanolubricants

The variance analysis of the response parameters was done by analyzing the influence of the nanoparticle as included in the obtained results. The analysis was

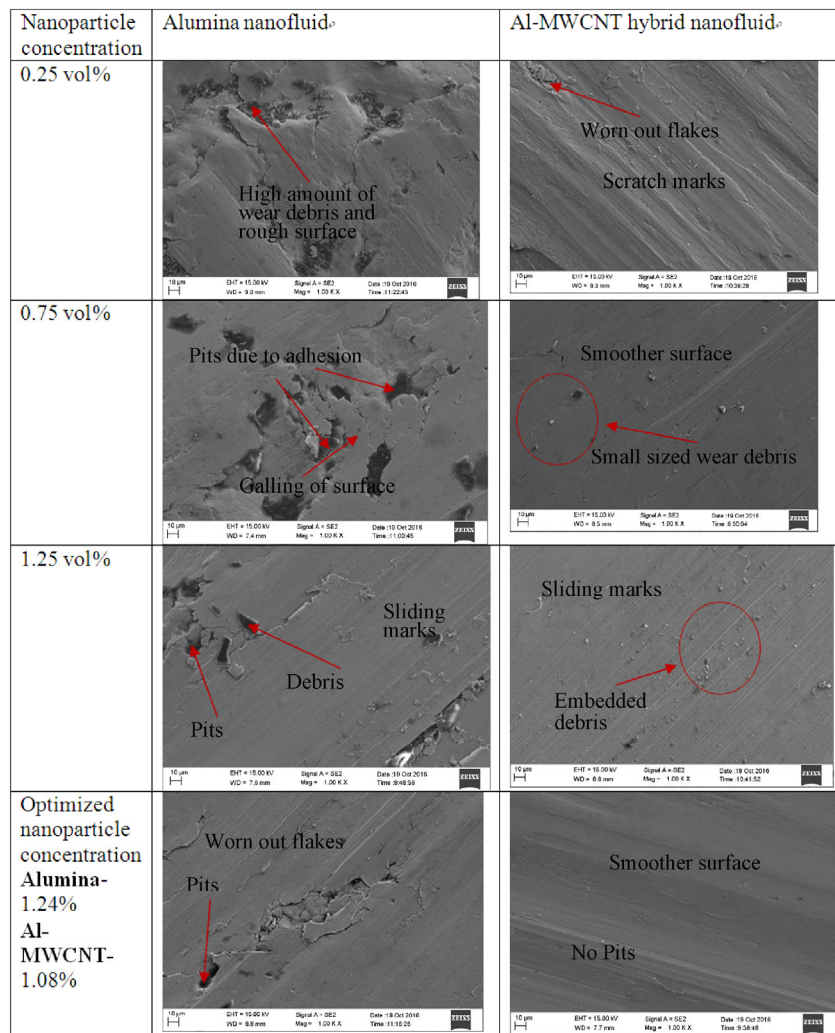


**Fig. 10** FESEM images of sliding surface of pins achieved during pin-on-disc tribology testing.



carried out at a confidence level of 95%, corresponding to a 5% significance level. Tables 3 and 4 show the ANOVA results of *T* and VB, respectively for the alumina nanofluids. The tables' last column names the influence of the variation of the input variables on the response parameter (output) as "significant" or "non-significant". It was found that the machining input variable np affects significantly the nodal temperature and the tool flank wear. The ANOVA results for *T* and VB of the alumina-MWCNT hybrid nanofluids are shown in Tables 5 and 6, respectively. The results clearly indicate that the np and its interaction with the cutting speed have a significant effect on *T* and VB.

**Table 3** ANOVA table of nodal temperature (*T*) for Alumina nanofluid.

Source	Sum of squares	DF	Mean square	F-value	Prob.	Remarks
Model	41779.75	14	2984.27	32.06	< 0.0001	Significant
A- <i>v</i>	630.75	1	630.75	6.78	0.0231	Significant
B- <i>f</i>	9571.10	1	9571.10	102.82	< 0.0001	Significant
C- <i>d</i>	24724.84	1	24724.84	265.62	< 0.0001	Significant
D- <i>np</i>	1060.32	1	1060.32	11.39	0.0055	Significant
AB	197.40	1	197.40	2.12	0.1710	
AC	1459.24	1	1459.24	15.68	0.0019	Significant
AD	2475.06	1	2475.06	26.59	0.0002	Significant
BC	14.44	1	14.44	0.16	0.7006	
BD	1.44	1	1.44	0.015	0.9031	
CD	6.50	1	6.50	0.070	0.7960	
A <sup>2</sup>	95.39	1	95.39	1.02	0.3314	
B <sup>2</sup>	195.75	1	195.75	2.10	0.1726	
C <sup>2</sup>	984.04	1	984.04	10.57	0.0069	Significant
D <sup>2</sup>	4.36	1	4.36	0.047	0.8323	
Residual	1116.99	12	93.08			
Lack of fit	1051.05	10	105.11	3.19	0.2623	Not significant
Pure error	65.94	2	32.97			
Cor total	42896.75	26				

**Table 4** ANOVA table of tool wear (*VB*) for Alumina nanofluid.

Source	Sum of squares	DF	Mean square	F-value	Prob.	Remarks
Model	25945.09	14	1853.22	18.88	< 0.0001	Significant
A- <i>v</i>	555.42	1	555.42	5.66	0.0348	Significant
B- <i>f</i>	6872.22	1	6872.22	70.01	< 0.0001	Significant
C- <i>d</i>	14309.23	1	14309.23	145.77	< 0.0001	Significant

(Continued)

Source	Sum of squares	DF	Mean square	F-value	Prob.	Remarks
D- <i>np</i>	889.41	1	889.41	9.06	0.0109	Significant
AB	75.00	1	75.00	0.76	0.3992	
AC	18.49	1	18.49	0.19	0.6720	
AD	405.62	1	405.62	4.13	0.0648	
BC	9.00	1	9.00	0.092	0.7672	
BD	0.93	1	0.93	9486	0.9240	
CD	1.49	1	1.49	0.015	0.9040	
A <sup>2</sup>	782.52	1	782.52	7.97	0.0154	Significant
B <sup>2</sup>	484.97	1	484.97	4.94	0.0462	Significant
C <sup>2</sup>	650.87	1	650.87	6.63	0.0243	Significant
D <sup>2</sup>	4.51	1	4.51	0.046	0.8340	
Residual	1177.99	12	98.17			
Lack of fit	1136.59	10	113.66	5.49	0.1638	Not significant
Pure error	41.39	2	20.70			
Cor total	27123.08	26				

**Table 5** ANOVA table of nodal temperature (*T*) for Al-MWCNT hybrid nanofluid.

Source	Sum of squares	DF	Mean square	F-value	Prob.	Remarks
Model	36797.66	14	2628.40	15.81	< 0.0001	Significant
A- <i>v</i>	1223.87	1	1223.87	7.36	0.0188	Significant
B- <i>f</i>	9400.30	1	9400.30	56.54	< 0.0001	Significant
C- <i>d</i>	19840.25	1	19840.25	119.32	< 0.0001	Significant
D- <i>np</i>	1050.24	1	1050.24	6.32	0.0272	Significant
AB	74.39	1	74.39	0.45	0.5162	
AC	592.31	1	592.31	3.56	0.0835	
AD	2005.36	1	2005.36	12.06	0.0046	Significant
BC	10.60	1	10.60	0.064	0.8049	
BD	392.54	1	392.54	2.36	0.1504	
CD	4.95	1	4.95	0.030	0.8659	
A <sup>2</sup>	588.06	1	588.06	3.54	0.0845	
B <sup>2</sup>	347.18	1	347.18	2.09	0.1741	
C <sup>2</sup>	604.15	1	604.15	3.63	0.0809	
D <sup>2</sup>	24.36	1	24.36	0.15	0.7086	
Residual	1995.25	12	166.27			
Lack of fit	1946.25	10	194.63	7.94	0.1169	Not significant
Pure error	49.00	2	24.50			
Cor total	38792.91	26				

**Table 6** ANOVA table of tool wear (VB) for Al-MWCNT hybrid nanofluid.

Source	Sum of squares	DF	Mean square	F-value	Prob.	Remarks
Model	23371.28	14	1669.38	15.27	< 0.0001	Significant
A- <i>v</i>	732.42	1	732.42	6.70	0.0237	Significant
B- <i>f</i>	6016.19	1	6016.19	55.03	< 0.0001	Significant
C- <i>d</i>	12697.76	1	12697.76	116.15	< 0.0001	Significant
D- <i>np</i>	720.91	1	720.91	6.59	0.0246	Significant
AB	47.61	1	47.61	0.44	0.5218	
AC	379.08	1	379.08	3.47	0.0872	
AD	1171.35	1	1171.35	10.72	0.0067	Significant
BC	6.79	1	6.79	0.062	0.8075	
BD	251.22	1	251.22	2.30	0.1554	
CD	3.17	1	3.17	0.029	0.8677	
A <sup>2</sup>	352.84	1	352.84	3.23	0.0976	
B <sup>2</sup>	213.11	1	213.11	1.95	0.1879	
C <sup>2</sup>	374.64	1	374.64	3.43	0.0889	
D <sup>2</sup>	20.83	1	20.83	0.19	0.6702	
Residual	1311.81	12	109.32			
Lack of fit	1280.45	10	128.05	8.17	0.1140	Not significant
Pure error	31.36	2	15.68			
Cor total	24683.09	26				

Equations (4) and (5) represent the regression model of the alumina nanofluids for values of the nodal temperature (*T*), tool flank wear (VB), coefficient of determination (*R*<sup>2</sup>) and adjusted *R*<sup>2</sup> equal to 97.40, 95.66, 95.36, and 90.59, respectively. Moreover, the regression models of the alumina-MWCNT hybrid nanofluids for the values of *T* and VB with coefficient of determination (*R*<sup>2</sup>) and adjusted *R*<sup>2</sup> equal to 98.11, 96.05, 95.90, 91.44 respectively, are given in Eqs. (6) and (7):

$$\begin{aligned}
 T_{(alumina)} = & 26.3469 - 3.05542 \times v + 2261.67 \times f \\
 & + 257.347 \times d - 169.425 \times np - 5.85417 \times v \times f \\
 & + 2.12222 \times v \times d + 1.65833 \times v \times np - 158.333 \times f \times d \\
 & + 30 \times f \times np - 8.5 \times d \times np + 0.00469907 \times v^2 \\
 & - 3786.46 \times f^2 - 150.926 \times d^2 + 3.61667 \times np^2
 \end{aligned}
 \tag{4}$$

$$\begin{aligned}
 VB_{(alumina)} = & -15.571 - 3.34731 \times v + 1798.3 \times f \\
 & + 332.597 \times d - 82.3883 \times np + 3.60833 \times v \times f \\
 & + 0.238889 \times v \times d + 0.671333 \times v \times np - 125 \times f \times d \\
 & + 24.125 \times f \times np - 4.06667 \times d \times np \\
 & + 0.0134588 \times v^2 - 5959.9 \times f^2 - 122.745 \times d^2 \\
 & + 3.67667 \times np^2
 \end{aligned}
 \tag{5}$$

$$\begin{aligned}
 T_{(Al-MWCNT)} = & 138.212 - 4.53113 \times v + 1337.14 \times f \\
 & + 248.559 \times d - 192.995 \times np \\
 & + 3.59375 \times v \times f + 1.35208 \times v \times d \\
 & + 1.49271 \times v \times np - 135.677 \times f \times d \\
 & + 495.312 \times f \times np - 7.41667 \times d \times np \\
 & + 0.0116672 \times v^2 - 5042.64 \times f^2 \\
 & - 118.258 \times d^2 - 8.54792 \times np^2
 \end{aligned}
 \tag{6}$$

$$\begin{aligned}
 VB_{(Al-MWCNT)} = & 107.57 - 3.54046 \times v \\
 & + 1049.71 \times f + 196.181 \times d - 148.529 \times np \\
 & + 2.875 \times v \times f + 1.08167 \times v \times d \\
 & + 1.14083 \times v \times np - 108.542 \times f \times d \\
 & + 396.25 \times f \times np - 5.93333 \times d \times np \\
 & + 0.0090375 \times v^2 - 3950.78 \times f^2 \\
 & - 93.125 \times d^2 - 7.905 \times np^2
 \end{aligned}
 \tag{7}$$

The influence of the nanoparticle concentration on the various response variables is shown through the response surfaces, as depicted in Fig. 11 and Fig. 12 for the alumina and Al-MWCNT nanofluids, respectively. Figures 11(a) and 11(b) show that the lowest nodal temperature was recorded at the highest np% with lowest feed and at the highest np% with the lowest depth of cut. Furthermore, the lowest tool wear was observed at a combination of highest np% and lowest feed (Fig. 11(c)), and of highest np% and lowest cutting speed (Fig. 11(d)). Additionally, Figures 12(a) and 12(b) show that the lowest nodal temperature was recorded at a combination of the highest np% and lowest feed, and of the highest np% with lowest depth of cut using Al-MWCNT hybrid nanofluids. The lowest tool wear was observed with a combination of highest np% and lowest feed (Fig. 12(c)) and of highest np% and lowest cutting speed (Fig. 12(d)).

### 3.3 Optimized input variables for the response parameters

The optimal values of input machining variables

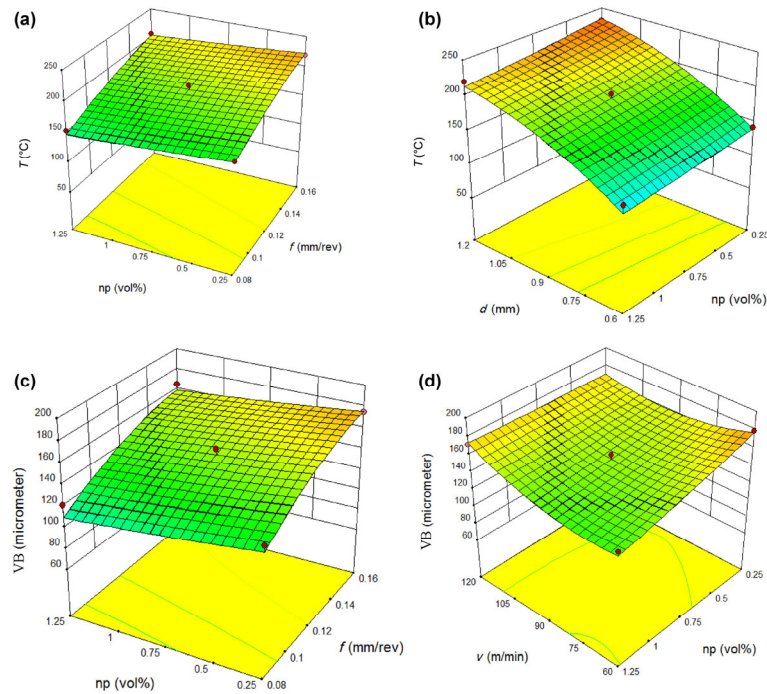


**Fig. 11** Estimated response surface plots for  $\text{Al}_2\text{O}_3$  nanoparticle concentration ( $np$ ) versus  $v$ ,  $f$ , and  $d$ .

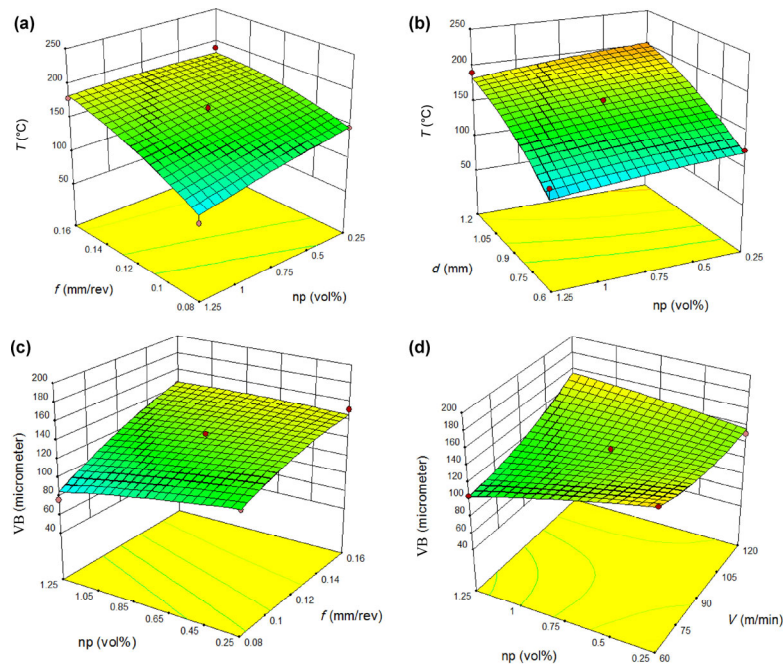


**Fig. 12** Estimated response surface plots for Al-MWCNT nanoparticle concentration ( $np$ ) versus  $v$ ,  $f$ , and  $d$ .

within their predefined range were determined during the turning process by minimizing both response parameters ( $T$  and  $VB$ ) independently. The goals, the input variables, and the response parameters' minimized values are summarized in Table 7 for the alumina and Al-MWCNT nanofluids.

### 3.4 Experimental validation

The validation of the optimized results was conducted through confirmation runs for the values of the machining input variables ( $v$ ,  $f$ ,  $d$ , and  $np$ ) as shown in Table 7. The average response was considered after

3 runs and compared to the optimized values. The experimental values corresponding to each response parameter are presented in Table 8. The validation results were in an acceptable range of  $\pm 4\%$  of the optimized values of the response parameters (Table 7). The variation of the validation experiments and the optimized results of  $T$  and  $VB$  for the alumina nanofluids were recorded at 2.7% and 1.54%, respectively. However, a variation of 3.00% and 3.39% of  $T$  and  $VB$  was recorded, respectively, for the Al-MWCNT hybrid nanofluids. This verifies that the experimental set-up and regression models were valid for a turning operation in the selected range of parameters selected for the alumina-base and hybrid (Al-MWCNT) nanofluids.

Table 8 shows a significant reduction in the nodal temperature and tool flank wear for the Al-MWCNT hybrid nanofluids compared to the alumina nanofluids. Also, mixing of MWCNT with alumina reduced the temperature from 83.53 to 60.67 °C and the average tool wear was also reduced from 65.39 to 58.16  $\mu\text{m}$ .

### 3.5 Nodal temperature

A significant reduction of 27.36% in nodal temperature with the use of Al-MWCNT hybrid nanofluid may be attributed to the superior thermal conductivity properties of the Al-MWCNT hybrid nanofluids compared to the alumina mixed nanofluids (Fig. 5). It is well known that a higher thermal conductivity represents a better heat extraction ability. Moreover, Al-MWCNT hybrid nanofluids showed better spreadability (lower contact angle) compared to alumina nanofluids at a carbide insert surface. This may contribute to providing the maximum wetting area per unit liquid volume for the heat extraction of the cutting tool, which could lower the tool's temperature. Furthermore, a lower friction coefficient was observed during the tribology testing of the Al-MWCNT hybrid nanofluids using a pin-on-disc tribometer. This lower friction may cause reduction in the heat generation during the relative motion of the tool and the work-piece. Hence, the mixing

**Table 7** Minimized response parameters for Alumina and Al-MWCNT nanofluid.

Nanofluid	Response parameter	Goal	Input variables				Minimized response value
			$v$ (m/min)	$f$ (mm/rev)	$d$ (mm)	$np$ (vol%)	
Al <sub>2</sub> O <sub>3</sub> nanofluid	Nodal temperature ( $T/^\circ\text{C}$ )	Minimize	60	0.082	0.6	1.15	81.29
	Tool flank wear ( $VB/\mu\text{m}$ )	Minimize	90	0.08	0.6	1.24	64.4
Al-MWCNT nanofluid	Nodal temperature ( $T/^\circ\text{C}$ )	Minimize	61.56	0.082	0.61	1.19	58.9
	Tool flank wear ( $VB/\mu\text{m}$ )	Minimize	69.1	0.08	0.64	1.08	56.25

**Table 8** Responses of validation experiments for Al<sub>2</sub>O<sub>3</sub> and Al-MWCNT nanofluid.

Nanofluid type	Response parameter	Test run	$v$ (m/min)	$f$ (mm/rev)	$d$ (mm)	$np$ (vol%)	Experimental value	Average
Al <sub>2</sub> O <sub>3</sub> nanofluid	$T$ ( $^\circ\text{C}$ )	1					85.89	<b>83.53</b>
		2	60	0.082	0.6	1.15	79.53	
		3					85.19	
	$VB$ ( $\mu\text{m}$ )	1					65.43	<b>65.39</b>
		2	90	0.08	0.6	1.24	64.86	
		3					65.88	
Al-MWCNT hybrid nanofluid	$T$ ( $^\circ\text{C}$ )	1					60.89	<b>60.67</b>
		2	61.56	0.08	0.62	1.19	59.94	
		3					61.18	
	$VB$ ( $\mu\text{m}$ )	1					57.95	<b>58.16</b>
		2	69.1	0.08	0.64	1.08	57.34	
		3					59.19	

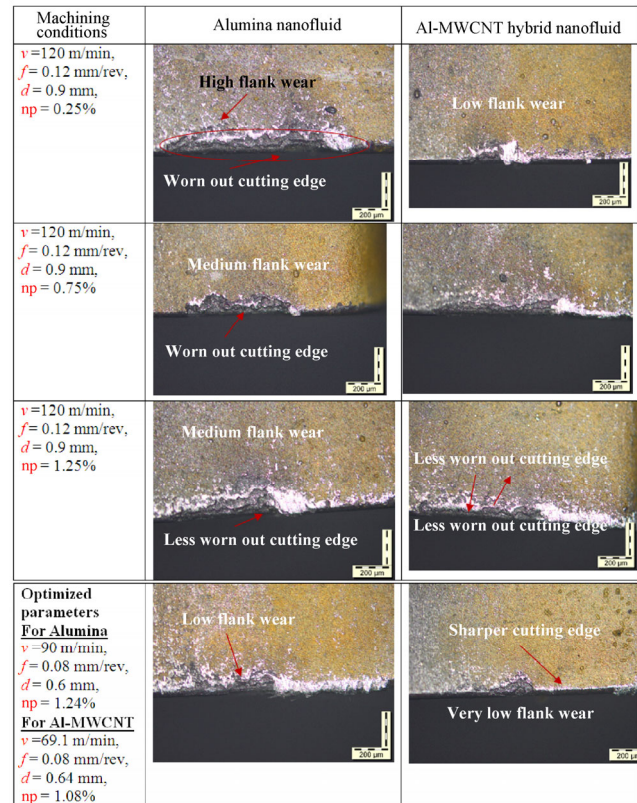


of MWCNT with alumina may improve the heat extraction and lubricating properties compared to the alumina nanofluids. The obtained results are in good agreement with previous investigations [24–26].

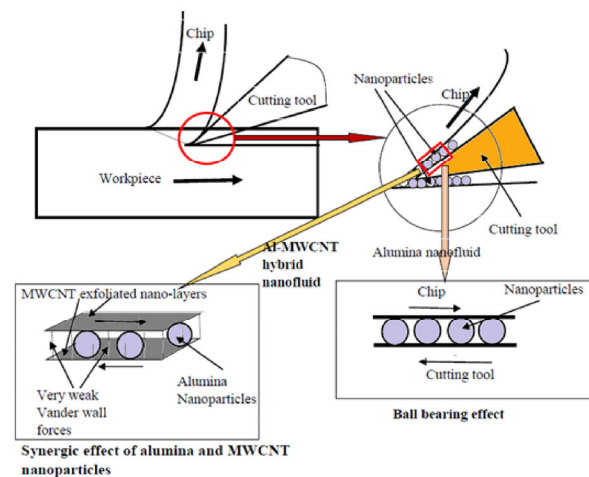
### 3.6 Tool flank wear

Figure 13 shows micrographs of the tool flank wear at 3 volumetric concentrations (0.25, 0.75, and 1.25 vol%) of alumina and Al-MWCNT nanofluids. It was found that the application of Al-MWCNT hybrid nanofluids recorded lower tool wear compared to alumina based nanofluids. Also, the increase of nanoparticle concentration reduced the tool flank wear possibly due to the reduced nodal temperature. The temperature generated at primary and secondary shear zone was primarily responsible for the tool wear. In the case of turning with Al-MWCNT hybrid nanofluids the tool edge retained its hardness for longer machining time due to a lower nodal temperature and thus partially reduced the flank wear compared to the alumina nanofluids.

It is known that the presence of alumina nanoparticles in cutting fluids generates ball bearing effect between the sliding surfaces [33, 34]. Figure 14 illustrates the ball bearing effect of nanoparticles present in the cutting fluid. It was found that the blending of MWCNT with alumina nanoparticles has further reduced the friction coefficient between sliding surfaces due to a synergic effect of the hybrid nanoparticles and an improved performance of the hybrid nanofluids. The weak structure of MWCNT easily exfoliated due to the shearing action of the chip over the tool surface. This led to the formation of thin tribo-films between the sliding surfaces [33, 35]. Moreover, the thickness of the films and their effect was enhanced by the presence of higher number of nanoparticles at higher concentrations. Therefore, a reduction in the friction coefficient (Fig. 8) and in the wear (Fig. 9) was observed with hybrid nanofluids over the monotype alumina-based nanofluids. The tribology testing results show the mechanism of nanofluid behavior between the sliding surfaces (Fig. 14). The lower friction force due to the presence of MWCNT nanoparticles reduced the cutting force as well as the nodal temperature. Moreover, the hybrid nanofluids extracted the heat from the tool at a higher



**Fig. 13** Microscopic photographs of tool flank wear with alumina nanofluids and Al-MWCNT hybrid nanofluids at  $v=120$  m/min,  $f=0.12$  mm/rev,  $d=0.9$  mm and at optimized process parameters, respectively.



**Fig. 14** Synergic effect of alumina/MWCNT hybrid nanoparticles during relative motion between the sliding surfaces.

rate and retained the hardness for longer periods because of their higher spreadability (wettability) at the tool surface and superior thermal conductivity compared to the alumina nanofluids.

## 4 Conclusions

A hybrid nanocutting fluid with improved thermal and tribological properties was developed from blending MWCNT with alumina-based nanofluids in fixed volumetric proportions (10:90). The performance of the alumina-MWCNT hybrid nanolubricants as cutting fluids in turning operation under MQL technique in terms of tool flank wear and nodal temperature was compared to the alumina-based monotype lubricants. The following conclusions were drawn:

1. The mixing of MWCNT with alumina nanofluids enhanced the thermal conductivity (~2.6%) with the increase of nanoparticle concentration.

2. Testing of pin-on-disc tribometer of Al-MWCNT hybrid nanofluids showed lower friction coefficient (~0.09) compared to alumina nanofluids (~0.18).

3. The smallest contact angle (wettability) of Al-MWCNT and alumina nanofluids was recorded at 39.5° (1.25 vol%) and 41.9° (1.0 vol%), respectively, suggesting that the mixing of MWCNT with alumina improves the spreadability.

4. A significant reduction of 27.36% in the nodal temperature was achieved for Al-MWCNT hybrid nanofluids compared to alumina nanolubricants.

5. The use of Al-MWCNT hybrid nanofluids reduced the tool flank wear by 11% compared to alumina nanolubricants.

6. The hybridization of two different nanofluids improved their tribological properties, demonstrating the feasibility of their use as lubricant/cutting fluids. The optimized nanoparticle concentration (~1.08 vol%) of the Al-MWCNT hybrid nanofluids yielded the lowest tool flank wear making them potential candidates for turning of AISI 304 stainless steel.

So far, researchers have focused on lubricants containing monotype nanoparticles. To conclude, in this study we found that the mixing of MWCNT with alumina in a fixed volumetric ratio (10:90) improved its tribological and thermophysical properties. The optimization of the mixing ratio may additionally enhance these properties. Future studies on the optimization of the nanoparticle volume fraction, shape, and size may contribute to developing nanolubricants with improved tribological properties for the machining of hard-to-cut materials.

**Open Access:** The articles published in this journal are distributed under the terms of the Creative Commons Attribution 4.0 International License (<http://creativecommons.org/licenses/by/4.0/>), which permits unrestricted use, distribution, and reproduction in any medium, provided you give appropriate credit to the original author(s) and the source, provide a link to the Creative Commons license, and indicate if changes were made.

## References

- [1] Maruda R, Legutko S, Krolczyk G. Influence of minimum quantity cooling lubrication (MQCL) on chip formation zone factors and shearing force in turning AISI 1045 steel. *Applied Mechanics and Materials* **657**: 43–47 (2014)
- [2] Attanasio, Gelfi M, Giardini C, Remino C. Minimal quantity lubrication in turning: Effect on tool wear. *Wear* **260**: 333–338 (2006)
- [3] Maruda R, Legutko S, Krolczyk G. Effect of minimum quantity cooling lubrication (MQCL) on chip morphology and surface roughness in turning low carbon steels. *Applied Mechanics and Materials* **657**: 38–42 (2014)
- [4] Cantero J L, Ivarez J D, Ilez M H M, Mariñ N C. Analysis of tool wear patterns in finishing turning of Inconel 718. *Wear* **297**: 885–894 (2013)
- [5] Klocke F, Settineri L, Lung D, Priarone P C, Arft M. High performance cutting of gamma titanium aluminides: Influence of lubricoolant strategy on tool wear and surface integrity. *Wear* **302**: 1136–1144 (2013)
- [6] Maruda R W, Krolczyk G M, Feldshtein E, Nieslony P, Tyliczszak B, Pusavec F. Tool wear characterizations in finish turning of AISI 1045 carbon steel for MQCL conditions. *Wear* **372–373**: 54–67 (2017)
- [7] Sartori S, Ghiotti A, Bruschi S. Hybrid lubricating/cooling strategies to reduce the tool wear in finishing turning of difficult-to-cut alloys. *Wear* **376–377**: 107–114 (2017)
- [8] Sharma A K, Tiwari A K, Dixit A R, Singh R K. Novel uses of alumina-MoS<sub>2</sub> hybrid nanoparticle enriched cutting fluid in hard turning of AISI 304 steel. *Journal of Manufacturing Processes* **30**: 467–482 (2017)
- [9] Sharma A K, Tiwari A K, Dixit A R, Singh R K. Investigation into performance of SiO<sub>2</sub> nanoparticle based cutting fluid in machining process. *Materials Today: Proceedings* **4**: 133–141 (2017)
- [10] Tiwari A K, Ghosh P, Sarkar J. Investigation of thermal conductivity and viscosity of nanofluids. *Journal of Environmental Research and Development* **7(2)**: 768–777 (2012)

- [11] Vajjha R S, Das D K. A review and analysis on influence of temperature and concentration of nanofluids on thermo-physical properties, heat transfer and pumping power. *International Journal of Heat and Mass Transfer* **55**: 4063–4078 (2012)
- [12] Yang Y. Carbon nanofluids for lubricant application. PhD Thesis. University of Kentucky, United States, 2006.
- [13] Choi S U S, Zhang Z G, Yu W, Lockwood F E, Grulke E A. Anomalous thermal conductivity enhancement in nanotube suspensions. *Applied Physics Letters* **79**(14): 2252–2254 (2001)
- [14] Sharma A K, Tiwari A K, Dixit A R. Progress of nanofluid application in machining: A review. *Materials and Manufacturing Processes* **30**(7): 813–828 (2015)
- [15] Lee C G, Hwang Y J, Choi Y M, Lee J K, Choi C, Oh J M. A study on the tribological characteristics of graphite nano lubricants. *International Journal of Precision Engineering and Manufacturing* **10**(1): 85–90 (2009)
- [16] Reddy N S K, Rao P V. Experimental investigation to study the effect of solid lubricants on cutting forces and surface quality in end milling. *International Journal of Machine Tools and Manufacturing* **46**: 189–198 (2006).
- [17] Kaynak Y, Karaca H E, Noebe R D, Jawahir I S. Tool-wear analysis in cryogenic machining of NiTi shape memory alloys: A comparison of tool-wear performance with dry and MQL machining. *Wear* **306**: 51–63 (2013)
- [18] Singh R K, Sharma A K, Dixit A R, Tiwari A K, Pramanik A, Mandal A. Performance evaluation of alumina-graphene hybrid nano-cutting fluid in hard turning. *Journal of Cleaner Production*, doi:10.1016/j.jclepro.2017.06.104 (2017)
- [19] Amrita M, Srikant R R, Sitaramaraju A V. Performance evaluation of nanographite-based cutting fluid in machining process. *Materials and Manufacturing Processes* **29**: 600–605 (2014)
- [20] Yasar H S, Heris H Z, Shanbedi M. Influence of soluble oil-based TiO<sub>2</sub> nanofluid on heat transfer performance of cutting fluid. *Tribology International* **112**: 147–154 (2017)
- [21] Parás L P, Tijerina J T, Garza L, Cortés D M, Michalczewski R, Lapray C. Effect of CuO and Al<sub>2</sub>O<sub>3</sub> nanoparticle additives on the tribological behavior of fully formulated oils. *Wear* **332–333**: 1256–1261 (2015)
- [22] Roy S, Ghosh A. High speed turning of AISI 4140 steel using nanofluid through twin jet SQL system. In *ASME International Manufacturing Science and Engineering Conference*, Wisconsin, Madison, June 10–14, 2013.
- [23] Jingxuan G, Gary C B, David J S, Qian Z, Scott B J. Tribological properties of ZnO and WS<sub>2</sub> nanofluids using different surfactants. *Wear* **382–383**: 8–14 (2017)
- [24] Sarkar J, Ghosh P. A review on hybrid nanofluids: Recent research, development and applications. *Renewable and Sustainable Energy Reviews* **43**: 164–177 (2015)
- [25] Tanshen M R, Lee S, Kim J, Kang D, Noh J, Chung H, Jeong H, Huh S. Pressure distribution inside oscillating heat pipe charged with aqueous Al<sub>2</sub>O<sub>3</sub> nanoparticles, MWCNTs and their hybrid. *Journal of Central South University* **21**: 2341–2348 (2014)
- [26] Nine M J, Batmunkh M, Kim J H, Chung H S, Jeong H M. Investigation of Al<sub>2</sub>O<sub>3</sub>-MWCNTs hybrid dispersion in water and their thermal characterization. *Journal of Nano-science and Nanotechnology* **12**: 4553–4559 (2012)
- [27] Ahammed N, Asirvatham L G, Wongwises S. Entropy generation analysis of graphene-alumina hybrid nanofluid in multiport mini channel heat exchanger coupled with thermoelectric. *International Journal of Heat and Mass Transfer* **103**: 1084–1097 (2016)
- [28] Zhang Y, Li C, Jia D, Li B, Wang Y, Yang M, Hou Y, Zhang X. Experimental study on the effect of nanoparticle concentration on the lubricating property of nanofluids for MQL grinding of Ni-based alloy. *Journal of Materials Processing Technology* **232**: 100–115 (2016)
- [29] Abbasi S M, Rashidi A, Nemati A, Arzani K. The effect of functionalization method on the stability and the thermal conductivity of nanofluid hybrids of carbon nanotubes/gamma alumina. *Ceramic International* **39**: 3885–3891 (2013)
- [30] Kanthavel K, Sumesh K, Saravanakumar P. Study of tribological properties on Al/Al<sub>2</sub>O<sub>3</sub>/MoS<sub>2</sub> hybrid composite processed by powder metallurgy. *Alexandria Engineering Journal* **55**: 13–17 (2016)
- [31] Khandekar S, Sankar M R, Agnihotri V, Ramkumar J. Nano-cutting fluid for enhancement of metal cutting performance. *materials and manufacturing processes* **27**: 963–967 (2012)
- [32] Wasan D, Nikolov A, Kondiparty K. The wetting and spreading of nanofluids on solids: Role of the structural disjoining pressure. *Current Opinion in Colloid & Interface Science* **16**: 344–349 (2011)
- [33] Park K H, Ewald B, Kwon P Y. Effect of nano-enhanced lubricant in minimum quantity lubrication balling milling. *Journal of Tribology* **133**: 31803 (2011)
- [34] Sharma A K, Tiwari A K, Dixit A R. Improved machining performance with nanoparticle enriched cutting fluids under minimum quantity lubrication (MQL) technique: A review. *Materials today: Proceedings* **2**: 3545–3551 (2015)
- [35] Dai W, Kheireddin B, Gao H, Liang H. Roles of nanoparticles in oil lubrication. *Tribology International* **102**: 88–98 (2016)



**Anuj Kumar SHARMA.** He received his PhD degree in Mechanical Engineering in 2017 from Indian Institute of Technology (ISM) Dhanbad India. Presently he is associated with

SRM Institute of Science and Technology Tamil Nadu as Research Assistant Professor. His core areas of research include machining, machining tribology, nano-cutting fluids and minimum quantity lubrication (MQL) machining.



**Jitendra Kumar KATIYAR.** He received his PhD degree in Mechanical Engineering from Indian Institute of Technology Kanpur India in 2017. Presently he is associated with SRM

Institute of Science and Technology Tamil Nadu as Research Assistant Professor. His research interests are surface coatings, lubrication tribology, polymer tribology, micro/nano tribology, and engineering materials



**Shubrajit BHAUMIK.** He received his M.Tech degree from SRM University Tamil Nadu India. Presently he is working as an Assistant Professor in the Department of Mechanical Engineering,

SRM Institute of Science and Technology. He has been awarded with best presentation award in Malaysian International Tribology Conference 2015. His research interests are nano-lubricants, texturing, polymer tribology, etc., and is working closely with many industries in the field of tribology.



**Sandipan ROY.** He received his PhD degree in Aerospace Engineering and Applied Mechanics in 2017 from Indian Institute of Engineering Science and Technology Shibpur

India. Presently he is associated with SRM Institute of Science and Technology Tamil Nadu as Research Assistant Professor. His core areas of research include bio-materials, bio-tribology, biomechanics, and finite element analysis.